Electronic Supplementary Material (ESI) for Journal of Materials Chemistry B.

Electronic Supplementary Information

Design of Oriented Mesoporous Silica Films for Guiding Protein Adsorption States

Yadong Chai,[a] Yuri Maruko,[a] Zizhen Liu,[a] Motohiro Tagaya [*a]

[a] *Department of Materials Science and Technology, Nagaoka University of Technology,*

Kamitomioka 1603-1, Nagaoka, Niigata 940-2188, Japan

*** Author to whom correspondence should be addressed:**

Tel: +81-258-47-9345, Fax: +81-258-47-9300, E-mail: tagaya@mst.nagaokaut.ac.jp

Figure S1

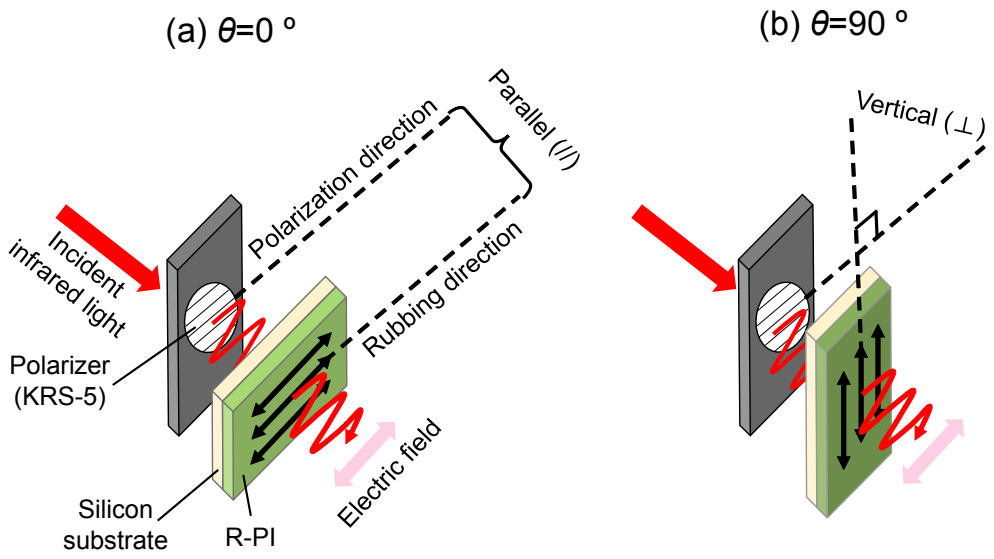

Figure S1. Illustration of the polarized FT-IR measurement systems. (a) the state of "polarization direction // rubbing direction" was named as "θ=0 °", and (b) the state of "polarization direction ⊥ rubbing direction" was named as "θ=90 °". The θ value was changed from 0 ° to 90 °.

Experimental procedure S1

The transmittance and haze value of films were measured by a UV−Vis absorption spectroscopy (V-730iRM, JASCO Corp.) and integrating sphere (ISF-834, JASCO Corp.) with the diameter of 60 mm. The total light transmittance (T_t) and diffusion rate (T_4) of the films and diffusion rate (T_3) of the instrument at the wavelength between 380 and 780 nm were calculated by the following **Equation (1)**.

$$T_x = \frac{\sum_{380}^{780} S(\lambda) y(\lambda) \tau_x(\lambda) d\lambda}{\sum_{380}^{780} S(\lambda) y(\lambda) d\lambda} \quad (1)$$

Here, $\tau_x(\lambda)$ is the transmittance spectrum in each measurement arrangement, $S(\lambda)$ is the spectral characteristic of the light source and $y(\lambda)$ is the visual sensitivity. The sample transmittance (T_d) by the following **Equation (2)**.

$$T_d = T_4 - T_3\left(\frac{T_t}{100}\right) \quad (2)$$

The haze value (Haze) was calculated by the following **Equation (3)**.

$$Haze = \frac{T_d}{T_t} \quad (3)$$

Figure S2

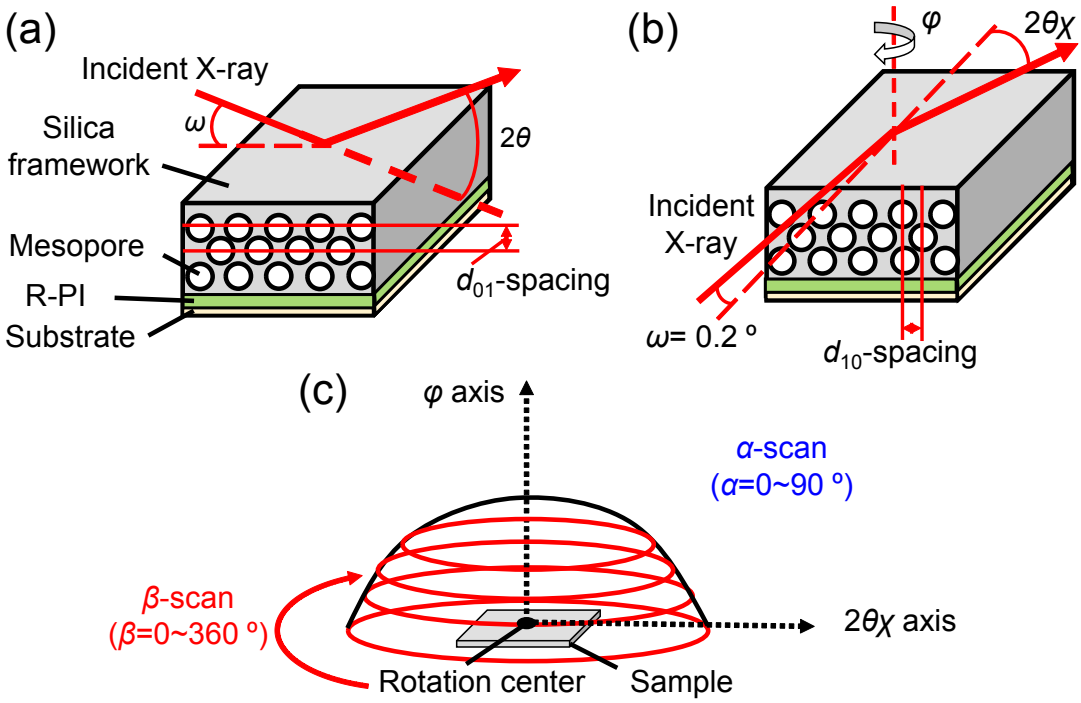

Figure S2. Illustration of various H-XRD measurement systems by (a) out-of-plane (2θ/ω-scan) where the ω and 2θ were changed to measure the lattice plane parallel to the sample surface, (b) in-plane (2$\theta\chi$/φ-scan) where the ω was fixed at 0.2 ° and 2$\theta\chi$ was changed to measure the lattice plane perpendicular to the sample surface and (c) pole figure methods (α-scan and β-scan) where the α and β were changed to evaluate the three-dimensional crystallographic orientation.

Figure S3

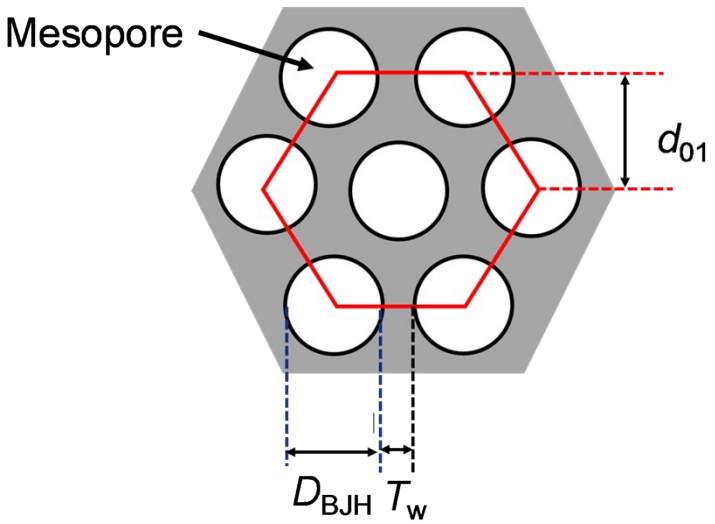

Figure S3. Illustration of the hexagonal mesopore structure for the calculation of the pore wall thickness (T_w).

Figure S4

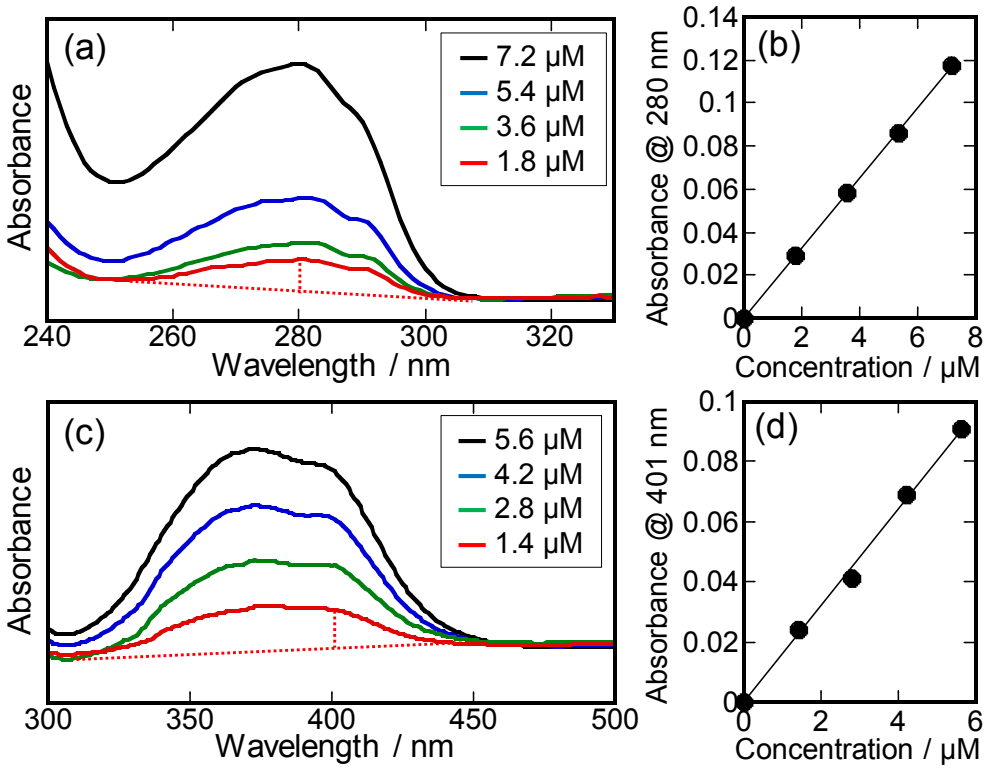

Figure S4. (a, c) UV-Vis absorption spectra and (b, d) calibration curves of the mono-component Lys (R = 0.9998) and (d) Myo (R = 0.9964) dispersed in the solution.

Figure S5

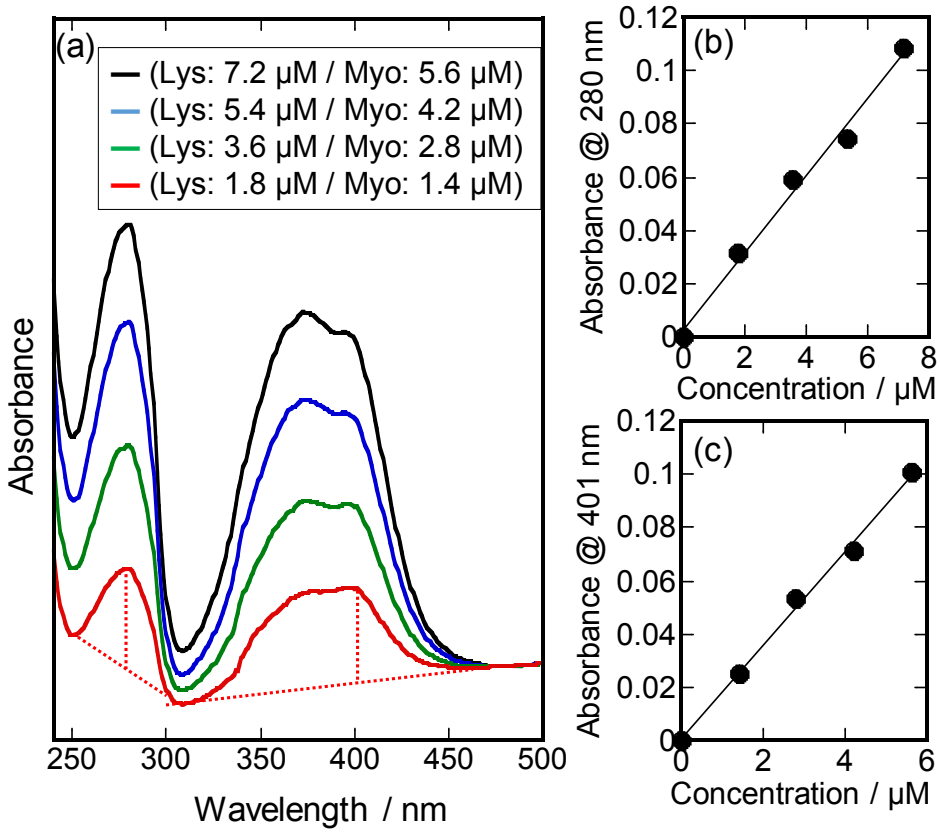

Figure S5. (a) UV-Vis absorption spectra of the two-component (Lys and Myo) solution and calibration curves of (b) Lys (R = 0.9824) and (c) Myo (R = 0.9955) dispersed in the solution.

Experimental procedure S2

The absorbance change in the different concentrations at 401 nm due to Myo was measured and calculated to obtain the calibration curve of Myo. Then, the absorbance change in the different concentration at 280 nm which derived from both Lys and Myo was calculated, so that the absorbance of Lys in the two-component solution was calculated by the following **Equation (4)**.

$$A_{Lys} = A_{280} - (A_{401} \times \frac{A_{M-280}}{A_{M-401}}) \quad (4)$$

where $A_{M\text{-}280}$ and $A_{M\text{-}401}$ were the absorbance of Myo in the mono-component solutions, A_{280} and A_{401} were the absorbance of Myo in the two-component solutions.

The amount of adsorbed proteins on the films were measured by the change in the concentration of proteins in the solution before and after the reaction. The concentrations of proteins were calculated by the calibration curve. The adsorption amounts (M (nmol/cm^2)) and ratios (R (%)) of Lys and Myo on the films were calculated by the following **Equation (5)** and **(6)**.

$$M = \frac{C_0 \times 0.003 - C \times 0.004}{5.76} \quad (5)$$

$$R = \frac{C_0 \times 0.003 - C \times 0.004}{C_0 \times 0.003} \quad (6)$$

where C_0 (μM) and C (μM) were the concentrations of proteins in the solutions before and after the reaction, the volumes of the protein solution before and after were 0.003 L and 0.004 L and the reaction areas of the films were 5.76 cm^2.

Figure S6

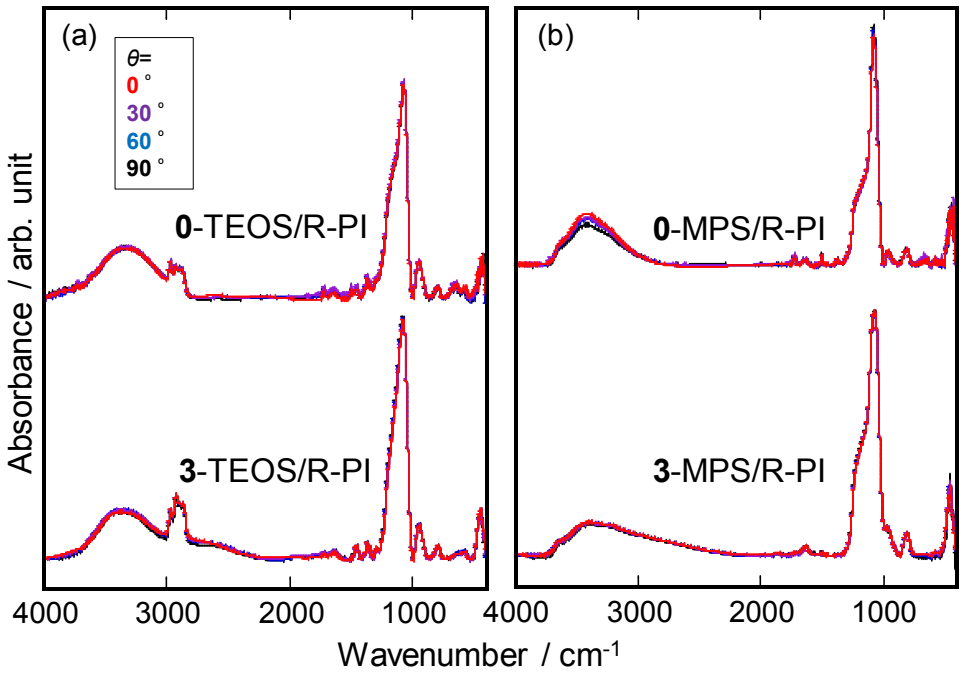

Figure S6. Polarized FT-IR spectra of (a) **0**-TEOS/R-PI and **3**-TEOS/R-PI, and (b) **0**-MPS/R-PI and **3**-MPS/R-PI.

Figure S7

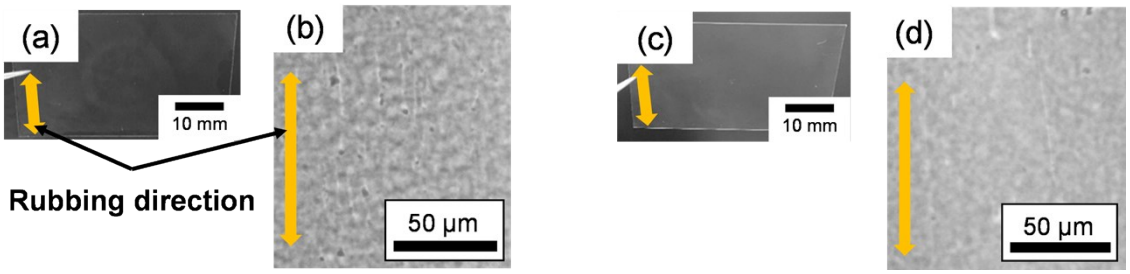

Figure S7. Photographs of (a) **0**-TEOS/R-PI and (c) **3**-TEOS/R-PI, and microscope photographs of (b) **0**-TEOS/R-PI and (d) **3**-TEOS/R-PI.

Figure S8

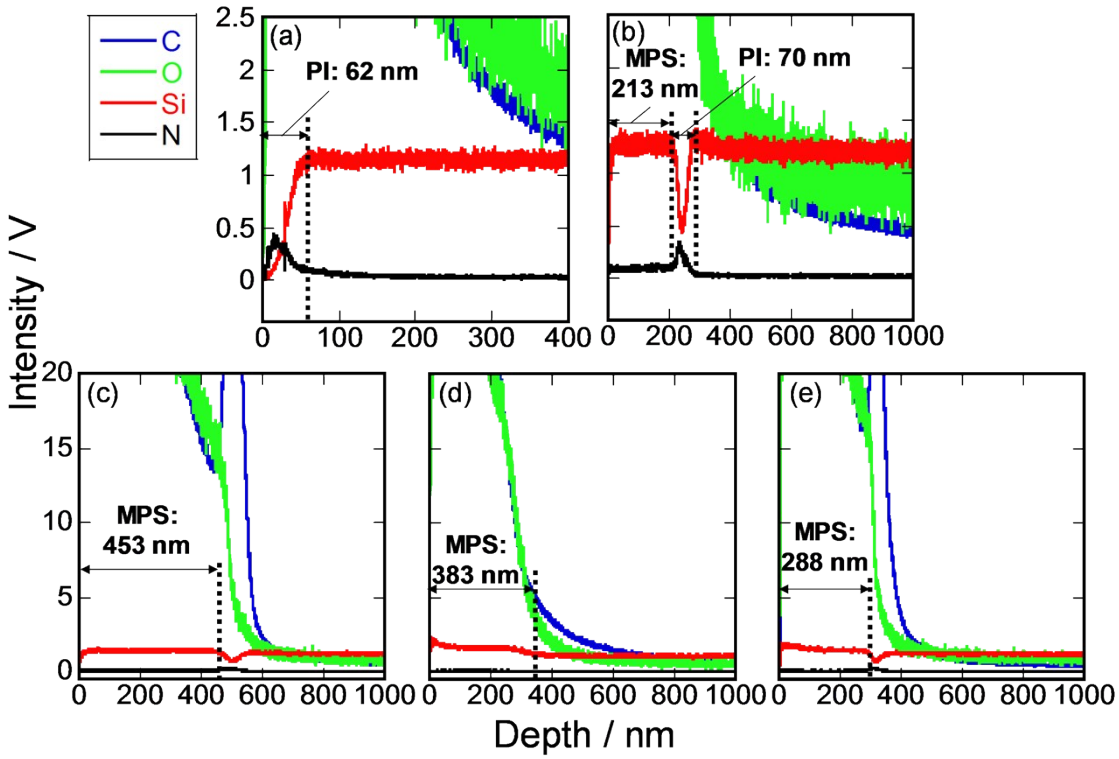

Figure S8. Depth profiles of (a) PI, (b) **0**-MPS/R-PI, (c) **2**-MPS/R-PI, (d) **3**-MPS/R-PI and (e) **4**-MPS/R-PI.

Figure S9

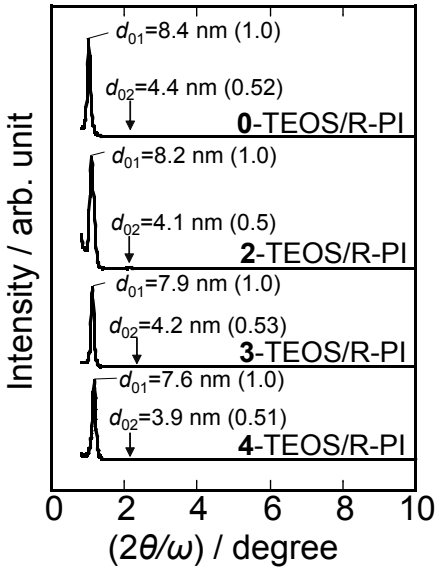

Figure S9. Out-of-plane XRD patterns of TEOS/R-PI films. Inset values were d_{01}- and d_{02}-spacing and their ratios by standardizing d_{01}-spacing value to be 1.

Figure S10

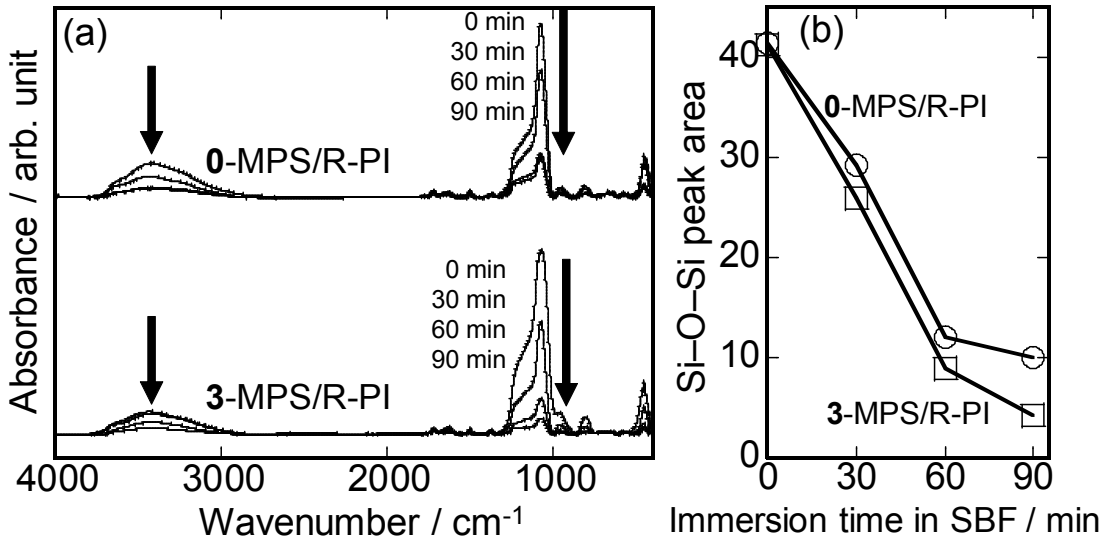

Figure S10. (a) FT-IR spectral and (b) Si–O–Si (996–1324 cm^{-1}) peak area changes of **0**-MPS/R-PI and **3**-MPS/R-PI with the immersion time in SBF.

Figure S11

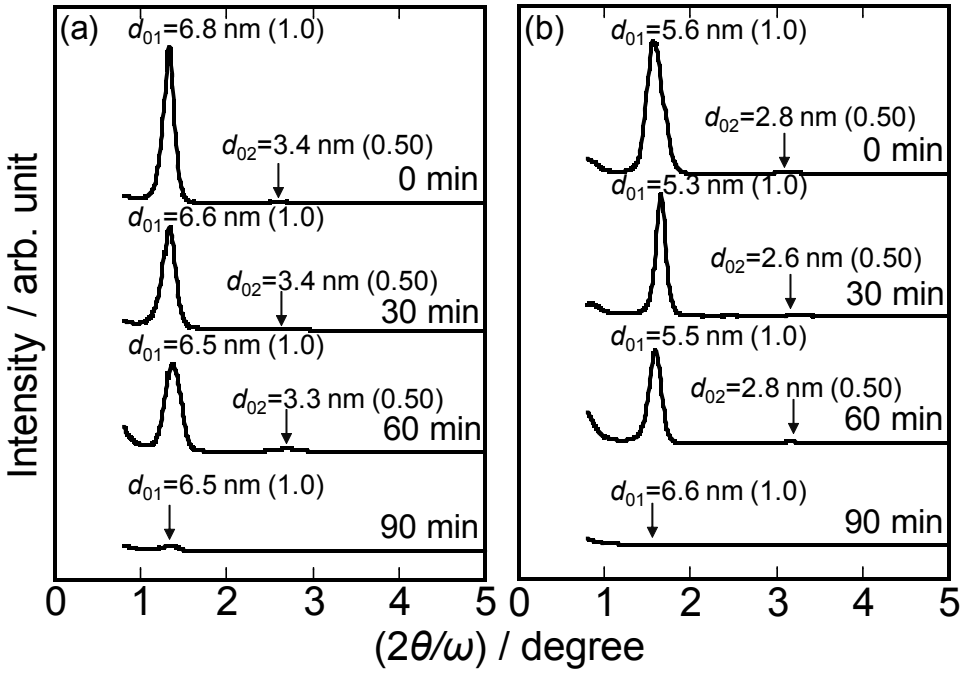

Figure S11. Out-of-plane XRD patterns of (a) **0**-MPS/R-PI and (b) **3**-MPS/R-PI with the immersion time in SBF.

Figure S12

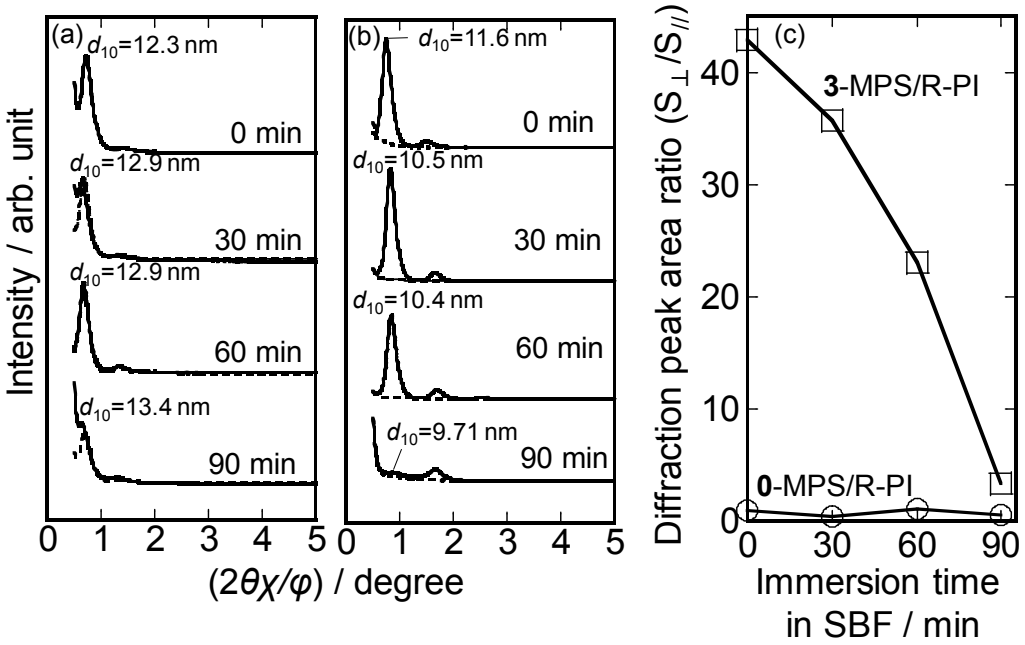

Figure S12. In-plane XRD patterns of (a) **0**-MPS/R-PI and (b) **3**-MPS/R-PI. The solid and dotted lines indicate the states as "X-ray incident ⊥ rubbing direction" and "X-ray incident // rubbing direction", respectively. (c) Diffraction peak area ratio ($S_\perp/S_{//}$) changes with the immersion time in SBF.

Figure S13

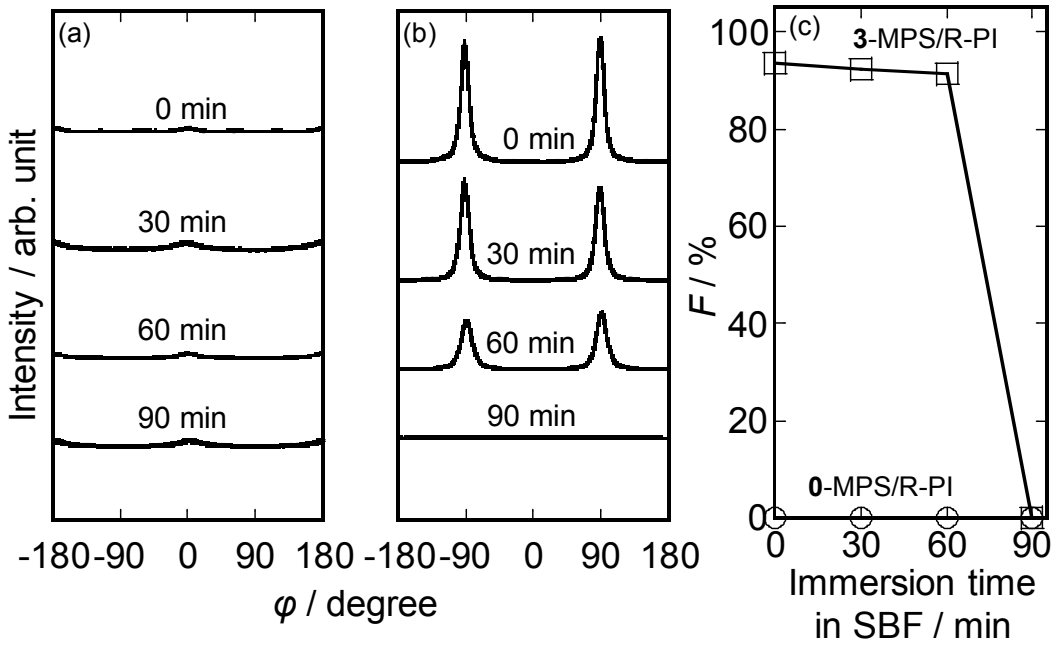

Figure S13. In-plane XRD *φ*-scan profiles of (a) **0**-MPS/R-PI and (b) **3**-MPS/R-PI, and (c) the orientation degree (*F*) changes with the immersion time in SBF.

Figure S14

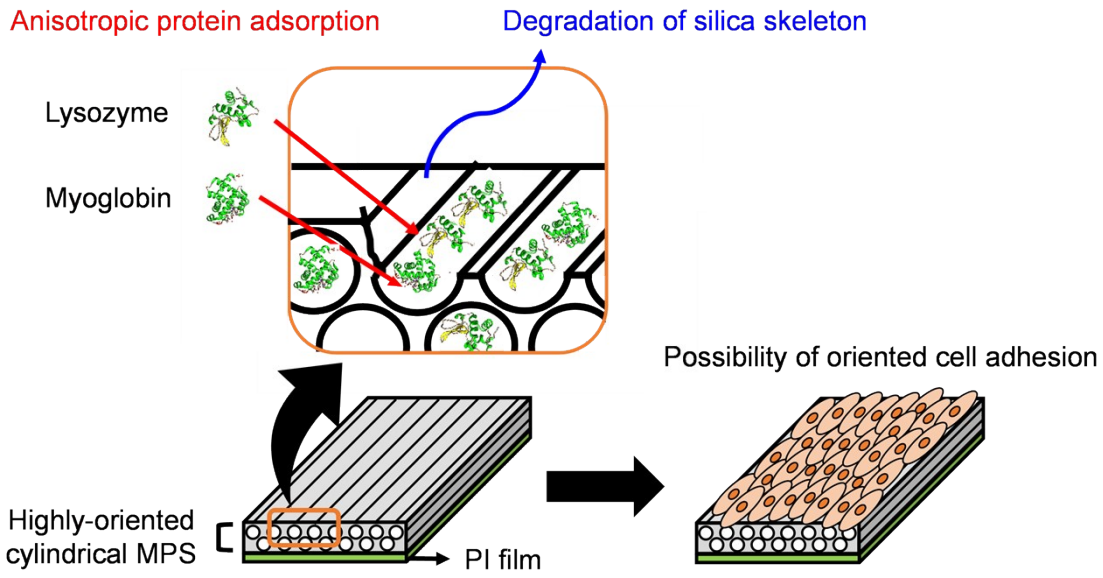

Figure S14. Illustration of the surface degradation of the highly-oriented cylindrical MPS film in biological solution to provide the oriented adsorption shapes of the proteins, leading to the oriented cell adhesion.